



## EXPLORING THE IMPACT OF WATER LEVEL VARIATIONS ON MODEL RIVER BANKS COMPOSED OF DIFFERENT SOIL TYPES A FLUME-BASED INVESTIGATION

ADIL M.R.<sup>1</sup>, KHATUN S.<sup>2</sup>, JAMAL M.<sup>1\*</sup>, JHA S.<sup>3</sup>, MEHTA D.<sup>4</sup>

<sup>1\*</sup> Assistant Professor, Department of Civil Engineering Aliah University,  
Kolkata, India

<sup>2</sup> Associate Professor, Department of Civil Engineering Aliah University, Kolkata, India

<sup>3</sup> Assistant Professor, Department of Civil Engineering, L. D. College of Engineering,  
Ahmedabad, India,

<sup>4</sup> Assistant Professor, Department of Civil Engineering, Dr. S. & S. S.  
Gandhy Government Engineering College, Surat, India

(\*) [jamalmohsin15@gmail.com](mailto:jamalmohsin15@gmail.com)

---

Research Article – Available at <http://larhyss.net/ojs/index.php/larhyss/index>  
Received October 12, 2024, Received in revised form May 28, 2025, Accepted June 1, 2025

---

### ABSTRACT

The objective of this study was to explore the pattern of failure and variation of pore water pressure in a river bank model consisting of medium cohesionless soil and silt dominated clay. To create the bank, a flume with dimensions of 550 cm in length, 150 cm in width, and 60 cm in depth was used. The length and depth of bank was 467 and 32 cm, having slope angle 33.64°. In this study, a reduced-scale distorted river modeling approach based on the Froude number was employed. The flume was scaled down by a factor of 1:250, while the depth of the model river bank was scaled down by a factor of 1:20. Two series were used in the study: Series-I and Series-II. For the physical model testing in Series-I, medium cohesionless soil with moisture values of 6% and 13% was taken. In Series-II, 10% and 15% water has taken for preparation of silt dominated clay bank. For the model bank (1V:1.5H), the same slope was used in both series. Drawdown of 0.5 and 0.8 times of height were taken in both series (Series-I and Series-II) for this study.

**Keywords:** River bank, Drawdown ratio, Water content, Pore pressure.

### INTRODUCTION

River bank failure and erosion are a universal problem and it is very problematic for those living on riverine areas (Remini, 2017; Mfoutou and Diabanguouaya, 2019; Riahi et al., 2020; Sarif et al., 2021).

Erosion and siltation of dams or hydraulic structures are closely related, as river bank erosion, or watersheds, can contribute to sedimentation, which accelerates the siltation process (Remini and Remini, 2003; Remini, 2010; Remini, 2017; Remini and Toumi, 2017). Erosion involves the removal of soil or rock from the land surface, often exacerbated by factors such as water flow, wind, or human activities. When this eroded material is transported into a water body like a river or reservoir, it can eventually accumulate behind a dam or in hydraulic structures, leading to siltation (Bougamouza et al., 2020). Siltation can significantly reduce the storage capacity of dams by filling reservoirs with sediments, thus impairing their functionality. Moreover, the rate of siltation is often increased when upstream erosion is more severe, particularly during heavy rainfall or flooding (Nezzal et al., 2015; Kouadio et al., 2018; Gassi and Saoudi, 2023; Remini, 2023). The ongoing sedimentation process can also affect water quality, the efficiency of water distribution, and overall management strategies for such infrastructure (Berzezel et al., 2023). Effective erosion control in the watershed can reduce the amount of sediment entering the dam, thus mitigating the long-term impacts of siltation.

The failure of the river bank is always having impact on social economic conditions of that particular areas (Kana Collins, 2017). In the West Bengal state, approximately 400 square kilometres spread across the 15 blocks in Malda, Murshidabad, and Nadia districts have experienced significant impact (Mondal and Patel., 2020; Waikhom et al., 2023; Chadee et al., 2024). The loss of nearly 2800 hectares of land can be attributed to erosion thus far (Ghosh, 2022; Islam et al., 2021; Sahu et al., 2024). Over the course of four decades, 700,000 individuals have been displaced from their homes (Das et al., 2017). A striking instance of this phenomenon occurred in the Shamsher Ganj block, where a 2.75 km stretch along the Ganga River eroded within a mere 50 days from August to September in 2020 (Islam et al., 2021; Mehta et al., 2022).

Due to the ensuing poverty and socioeconomic issues, river bank erosion in some Indian states deteriorates into a major environmental disaster that forces forced migration (Das et al., 2017; Mondal and Patel., 2020; Khatun et al., 2019; Verma et al., 2024). As a result, a growing corpus of scientific literature examines the stability and failure of various water front slopes, such as river banks. Understanding the causes of bank erosion is necessary to provide appropriate methods for measuring it and to propose mitigation strategies (Islam et al., 2023; Sen, 2008; Mehta et al., 2023). The majority of catastrophic mass riverbank breaches in India are composed of alluvial or loamy sand and semi-cohesive material, typically failure happening as a result of the decrease in water level following a flood in the river (Parker et al., 2008; Karasu et al., 2023). One system that suffers from severe erosion and bank instability is the Mississippi Yazoo River Basin (Nardi et al., 2012). The stability of stream banks is largely dependent on the characteristics of the bank materials, and previous research has shown that these characteristics are frequently regionally varied (Rinaldi and Casagli, 1999; Osman and Thorne, 1988; Perez et al., 2023; Ertuğru et al., 2022; Chapokpour and Azamathulla, 2025).

Hydrostatic pressure (pore) is acknowledged as an element that impacts the stability of river banks (Li et al., 2022; Krzeminska et al., 2022; Gasparotto et al., 2022; Mehdi et al., 2023). In instances when the river stage experiences a rapid decrease due to either natural

or artificial causes, the seepage gradients cause additional pore pressures to arise, thus resulting in a reduction of both the effective stress and shear strength of the soil comprising the bank (Zhou et al., 2019; Karakurt et al., 2023; Achour et al., 2024; Sharma et al., 2023). It becomes possible for a mass failure event to be initiated if the pore pressure response is not dissipated before the destabilizing forces surpass the available shear strength (Tiwari et al., 2023; Parez et al., 2023; Duong et al., 2019;). The intensity of pore pressure change during drawdown is controlled by properties of the bank materials, hydraulic conditions, and rate of water level (Chen et al., 2011; Pandey et al., 2023; Camaj et al., 2024; Karaca et al., 2022; Kantharia et al., 2024)

Before beginning any river bank protection project, the literature emphasizes the need for a thorough laboratory investigation to analyse the failure patterns and fluctuations of pore water pressure within the bank. The output of the study can be used in designing any type of protection work on a river bank. Additionally, it attempts to evaluate the soil's capability for replicating bank failure in a lab environment, reflecting actual failure patterns. The study explores the impact of soil type, moisture content, and drawdown on the distribution of pore water pressure at various river stages, as well as changes in the position of failure and profile changes

## **METHODOLOGY**

The model bank was constructed in a manufactured flume that was available at Aliah University's hydraulic laboratory in Kolkata. In order to physically simulate the riverbank, Froude (F) similarity was employed. To prepare the model bank, a distorted scale with lengths of 1:250 and heights of 1:20 was utilized. There were two series in the experimental program: series-I and series II. For banks in the series-I model, medium cohesionless soil (sand) was used, with starting moisture values of 6% and 13%. Model banks for series-II were prepared using silt dominated clay soil with water content values of 10 and 15 percent. 1V:1.5H slope of bank has taken for this study and 0.5 and 0.8 ratio of drawdown were maintained in both series.

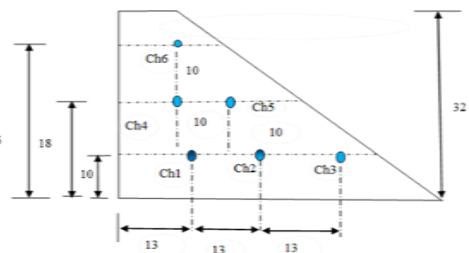
### **Model setup**

The model flume's measurements are roughly 550 cm long, 150 cm wide, and 60 cm deep. An adjacent seepage area is incorporated into this experimental flume along the bank's longitudinal sides. Two sets of pumps have been added in the setup to make testing for filling water. The seepage tank's water level is kept constant by a 5L/s pump, which replicates the water table inside the bank. Concurrently, a 32 liters per second pump is utilized to produce channel flow for filling the water in model flume. Trial experiments were conducted to assess the pump capacity with great care to achieve drawdown ratios from the high flood level, which is necessary to observe failure circumstances. Interestingly, the setup's arrangement is intended to closely resemble real-world situations. The images of real setup of experimental model flume were shown in Fig. 1a.

The variations in pore water pressure along the cross section of the model river bank were measured using a Pore water pressure monitoring system with Sensors and Data-logger shown in Fig. 1b. Six channel of pore pressure measuring device placed at different locations on the bank during the construction of the model river bank. The other ends of these tubes are connected to the sensors for measuring the pressure. The working range of these pore pressure devices laying between 0.01 kPa to 4 kPa. The positions of these sensors pipe within the bank are illustrated in Fig. 1b.



(a)



(b)

**Figure 1: Picture of the model flume (a) Photographs of flume (b) Photographic and schematic view of pore pressure device and location for pore water pressure measurement**

### Dimensions of the bank

The experiments were carried out to investigate the effects of different drawdown ratios and bank materials on the failure mechanism and profile of a river bank. For each series, a physical model was created in a lab flume with the same bank height and a constant 1V:1.5H slope. Table 1 provides specifics on the model bank geometry's dimensions, while Fig. 2 provides illustrations of the bank geometries and slopes.

**Table 1: Dimensions of the bank**

Slope	Angle (Degree)	Height (cm)	Width (cm)
1V:1.5H	33.69	32	58

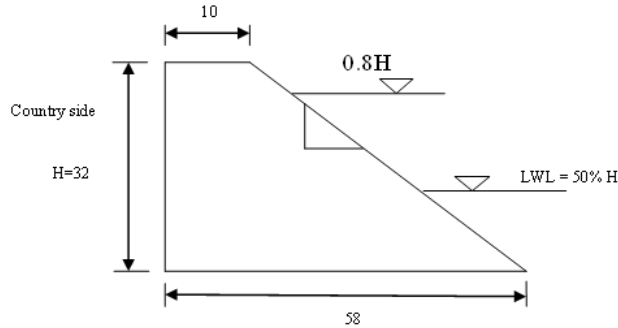


**Figure 2: Bank Geometry (Dimensions in cm according to Table 1)**

### Material used for model bank

This experimental study employed two types of soil. Cohesionless soil, or sand, was utilized in Series-I to create the model bank. The banks of Series-II were model banks built on silt dominated soil.

### Non-Cohesive Soil

Medium sand that was collected from the nearby location was used as bank material in this investigation (Series-I). Table 2 presents the fundamental geotechnical characteristics of the bank material in accordance with Indian Standards.

**Table 2: Properties of cohesionless soil**

Properties	Range
Specific gravity	2.61
Friction angle ( $\phi$ ) for bank material for 6% moisture	31.20°
Friction angle ( $\phi$ ) for bank material for 13% moisture	33.30°
Unit wt. ( $\gamma_t$ ) (kN/m <sup>3</sup> ) at moisture 6%	15.12
Unit wt. ( $\gamma_t$ ) (kN/m <sup>3</sup> ) at moisture 13%	16.39

**Silty clay**

The soil type used to prepare the model bank in Series-II is silty clay. It was gathered in Kaliachak-III, Malda, West Bengal, India, from the Ganga River. The soil's engineering properties have been identified in accordance with the process outlined in the Indian Standard Code Index. Table 3 presents the properties in tabular form.

**Table 3: Geotechnical properties of the soil**

Properties	Values
Specific Gravity	2.65
Grain Size Distribution	Silt = 70.1% Clay = 24.7% Sand=5.2%
Silt Factor	0.229
(Cu)	3.75
(Cc)	0.51
Permeability in cm/s	$2.6 \times 10^{-7}$
Cohesion and friction angle	$C = 0.9 \text{ kPa}$ $\phi = 18.2^\circ$
Liquid Limit	43.6.2
Plastic Limit	26.54

**Preparation of physical model for testing**

A precise methodology was utilized for both series-I and series-II in order to guarantee the specified attributes of the model embankments. Non-cohesive model embankments were intricately constructed in series-I using a consistent compaction. The primary bulk densities, adjusted according to water content (WC) percentages of 13 and 6 were an immediate outcome of this procedure. Achieving the desired density necessitated the systematic construction of the banks in three tiers, each subjected to 25 impacts. Series-II focused on model banks composed of silty dominated clay soil having 10% and 15% moisture for achieving the target unit weight of  $17.6 \text{ kN/m}^3$  and  $18.56 \text{ kN/m}^3$ . Throughout the preparation procedure, each layer received a compaction energy of  $0.209 \text{ kg/cm}^2$ , guaranteeing accuracy and uniformity in the model's creation (Fig 3). Both series meticulous preparation techniques sought to provide realistic riverbank models that would enable a thorough examination of the impact of different variables on the failure of bank.



**Figure 3: Model Bank prepared in flume**

Upon completion of setting up the model riverbank, the measuring gauge was positioned onto the bank's surface to acquire the initial profile reading. The initial measurements were indicated by these measuring instruments. Subsequently, water will fill in tank through start of pump. The exterior valve was used to keep the water at a required level. Through the utilization of the floating technique, the velocity of the water flow on the surface was measured 6 cm/s. Subsequent to the flume operating for 60 minutes. In this investigation, two standing heights—0.5 and 0.8 of height were chosen for recession of water. The comprehensive experimental schedule is listed in the tables below (Tables 4 and 5).

**Table 4: Details of test for Series-I**

Material for bank preparation	Bank slope	Water content	Testing time	Height of the water	No. of trail
Cohesionless soil	1V: 1.5H	6%	30 min	50%	3
				80%	3
		13%		50%	3
				80%	3

**Table 5: Details of test for Series-II**

Material for bank preparation	Bank slope	Water content	Testing time	Height of the water	No. of trail
Silt dominated clay	1V: 1.5H	10%	30 min	50%	3
				80%	3
		15%		50%	3
				80%	3

## DETAIL DISCUSSIONS OF RESULTS

### Impact of drawdown and moisture content on model bank profile (Series-I)

Twelve model experiments were carefully carried out in this experimental series for a bank prepared with cohesionless soil, for drawdown ratios of 0.5 and 0.8 of the height. The starting water content of 6% and 13% were purposefully chosen to provide some variation in the properties of the soil. The different profiles for different cases are shown in Figs. 4,5,6 and 7. The model riverbank failed very little near its toe for 0.5 times height and moisture content of 6%.

On the contrary, the depletion of 0.8 of height led to a notable failure, resulting in the sliding of the soil mass at the center of the slope. It is noteworthy that, unlike the 0.5 time of height reductions, the 0.8 time of height reduction with a moisture level of 6% triggered the most prominent failure, irrespective of water content. This observation points to a greater susceptibility to failure in situations with more severe drawdown. It's noteworthy to notice that the slight increase in moisture content from 6% to 13% had no appreciable impact on the size of failures, regardless of whether drawdown was at 0.5H or 0.8H. This research's output sheds light on the intricate relationships that impact the stability of bank.

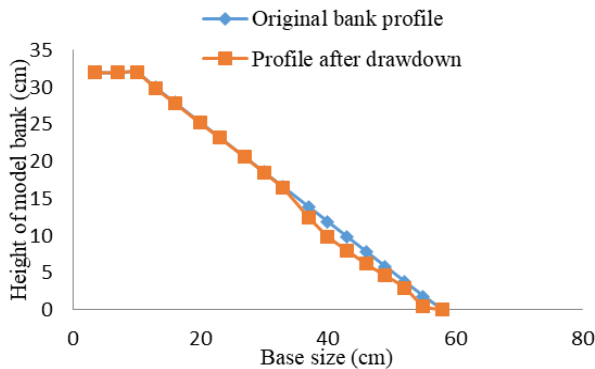


Figure 4: Profile of bank for water content 6% and water level 50%

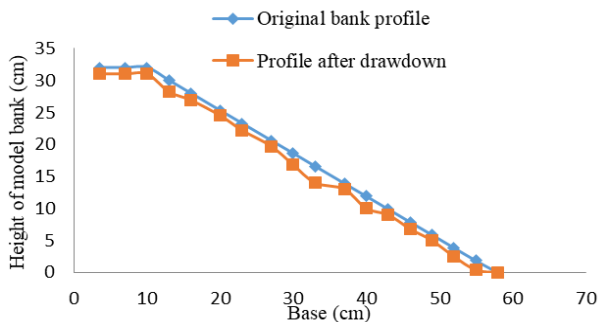
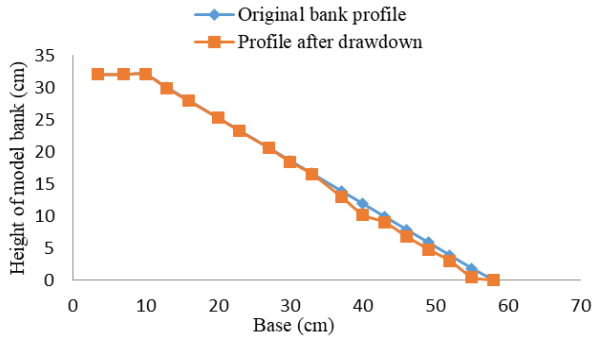
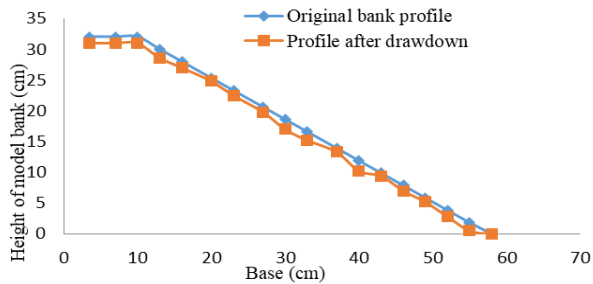


Figure 5: Profile of bank for water content 6% and water level 80%

*Exploring the impact of water level variations on model river banks composed of different soil types: A flume-based investigation*



**Figure 6: Profile of bank for water content 13% and water level 50%**



**Figure 7: Profile of bank for water content 13% and water level 80%**

One key takeaway from this experimental work was determining the failure location, failure time (Table 6). With water level 0.5 times of height, failure locations were found to be 20.92 cm and 11.4 cm from the bottom. Failures started to occur 27 and 32 seconds after the water recession, respectively, for 6% and 13% water content. These results go against the grain of traditional wisdom, implying that the start of bank failure is not always determined by the immediate aftermath of downturn. One important aspect affecting the temporal dynamics of bank stability is the pore water's outflow. Upon closer inspection, failures were evident at 28.72 cm and 21.9 cm from the bottom at an 80% H dip. For moisture concentrations of 6% and 13%, the commencement times were 26 and 37-seconds following drawdown started respectively. This illustrates the strong relationship between water content, drawdown height on stability of bank. The findings presented in this study enhance our comprehension of the complex temporal and spatial variations that govern the stability of riverbanks during drawdown. The expulsion of pore pressure also an important parameter to impact the stability.

**Table 6: Failure zone for bank prepared with cohesionless soil**

water content %	Water level	Failure from toe (cm)	Initiation time of failure d/d (sec)
6%	50%	20.9	27
	80%	28.72	26
13%	50%	11.4	32
	80%	21.9	37

**Variation of pore water pressure (Series-I)**

The sand used in the construction of the model bank had varying levels of moisture content, specifically 6% and 13%, and a slope of 1H:1.5V. The tank containing the model bank was then filled with water to two different heights, specifically 50%H and 80%H. The results of the experiment indicate that during the initial stage of drawdown, the pore water pressures in channels Ch1, Ch2, and Ch3 were measured to be 1.08, 1.40, and 1.27 kPa, respectively, for a moisture content of 13% and a water level at 80%H. In contrast, the upper channels, namely Ch4, Ch5, and Ch6, exhibited significantly lower pore water pressures, measured at 0.2, 0.45, and 0.10, respectively. These findings can be further examined in Figs. 8 and 9.

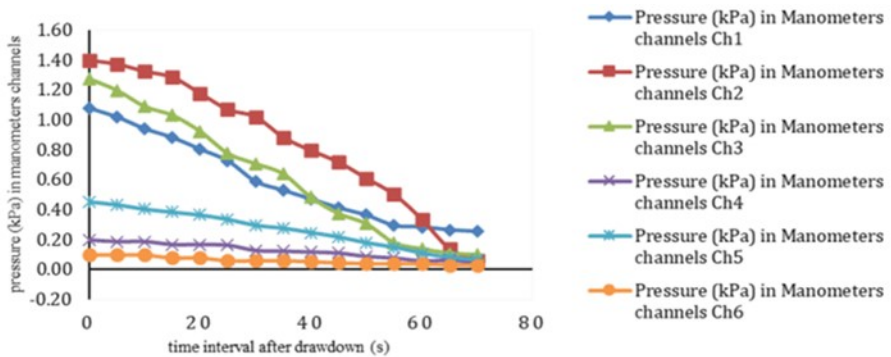


**Figure 8: Pore Water Pressure distribution of model bank in 13 % moisture content at drawdown ratio 80% H**

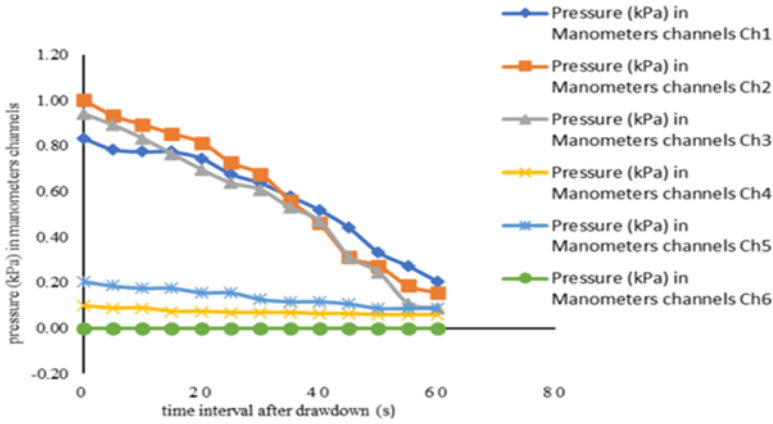


**Figure 9: Pore Water Pressure distribution of model bank in 13 % moisture content at drawdown ratio 50% H**

For a water content of 6% and a drawdown of 0.8H, the initial manometer readings were documented as 1.62, 1.81, 1.53, 0.28, 0.5, and 0.20 kPa for channels 1, 2, 3, 4, 5, and 6, respectively. These results of pore water pressure indicate that the combination of 6% moisture content and 80 % H drawdown generates a more precarious state for the slope. The bank displayed increased vulnerability to failure under the drawdown of 80 % H with a moisture content of 6%. As time progressed, the dissipation of pore water took place, and after 50 seconds, it was observed that the rate of dissipation was quicker in the model bank with 13% moisture content and 80%H drawdown compared to other scenarios, as illustrated in Figs. 10 and 11.

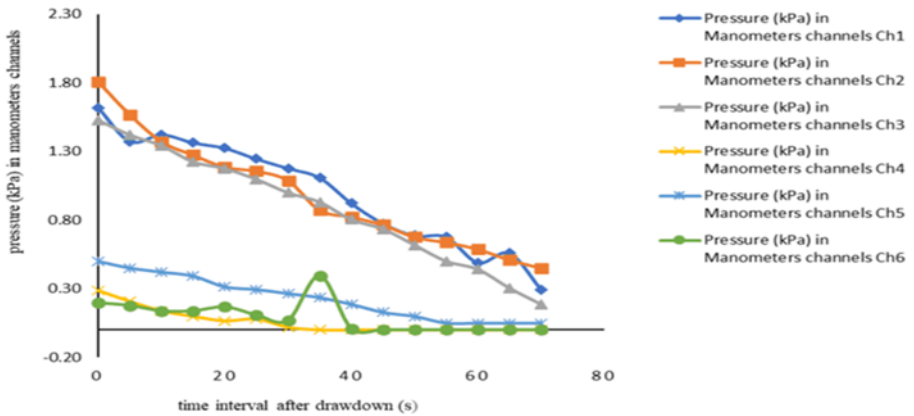


**Figure 10: Pore Water Pressure distribution of model bank in 6.0% moisture content at drawdown ratio 80% H**

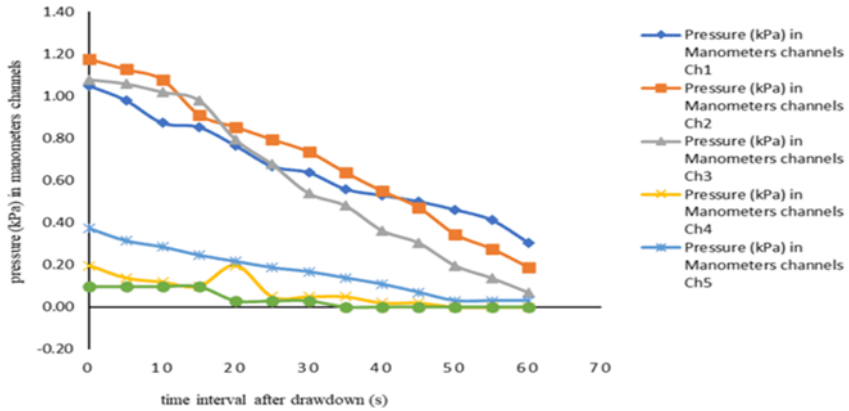


**Figure 11: Pore Water Pressure distribution of model bank in 6% moisture content at drawdown ratio 50% H**

**Impact of drawdown and moisture content on model bank profile (series-II)**

In this set of model banks made of silty clay, at 50% flow height, both 10% and 15% of the moisture contents showed some erosion. It is remarkable, nevertheless, that following the test, there were no discernible changes in slope. Because the changes in the topography of the bank were not significant, the profile for this specific test combination is not given.

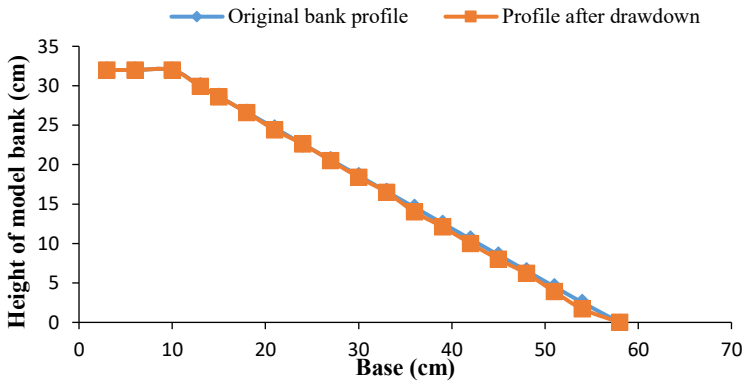


**Figure 12: Profile bank for water content 10% and water level 80%**

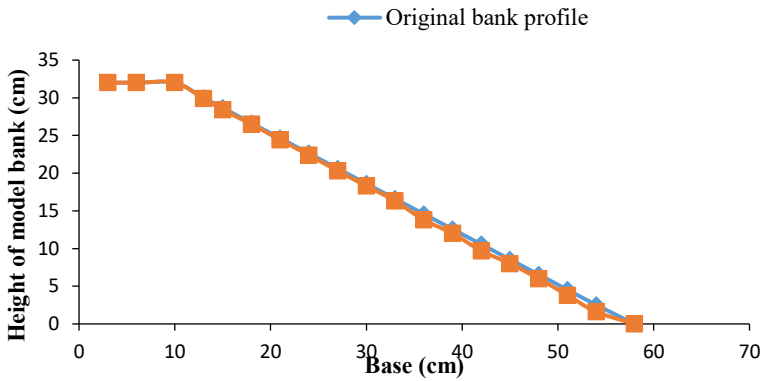


**Figure 13: Profile of bank for water content 15% and water level 80%**



**Figure 14: Failure crack**

As seen in Figs. 12, 13 and 14, partial erosion and the development of a longitudinal fracture happened at 0.8 times of height of flow. Furthermore, as Table 7 shows, it was found that the failure position for an 0.8 times height of drawdown began 16 and 21 cm from the bottom at intervals of 46 and 61 seconds, respectively. The properties of the silty clay soil have affected these observations significantly. Because the internal cohesive action of the bank material efficiently withstands the seepage pressures working on the bank during water outflow following drawdown, the forces causing bank failure have less of an impact on erosion and failure in silty dominated clay. The findings indicate that the sand-based bank exhibits a somewhat similar failure to what was seen on the field.

**Table 7: Location of failure for Series-II**

Water content %	Water level	Failure from toe (cm)	Initiation time of failure (sec)
10	50%	-	0
	80%	16	46
15	50%	-	0
	80%	21	61

**Variation of pore water pressure (Series-II)**

In the second set of experimental trials, a replica river bank was fabricated employing silty clay soil. The field density was simulated by maintaining the moisture content of the replica river bank at 10% and 15%, corresponding to 15.6 and 16.85 kN/m<sup>3</sup>, respectively. The drawdown ratio remained consistent with the previous experiments. It was observed that the pore water pressure in silty clay differed from that in banks made of sandy soil. For a moisture content of 15% and drawdown of 80%H and 50%H, channels such as Ch1 and Ch4 displayed minimal manometer readings, indicating the absence of pore water in the deeper section of the bank. Conversely, channels closer to the surface, such as Ch2, Ch3, and Ch5, exhibited significantly higher pore water pressures, measuring 2.49, 1.78, and 0.49 kPa, respectively (refer to Figs. 15 and 16). Furthermore, it was noted that pore water pressure did not dissipate easily from the replica bank. Measurements taken 50 seconds after drawdown showed only a 40% to 50% reduction in pore water pressure, which contradicted the quicker dissipation observed in the replica bank constructed with sandy soil in previous experiments.

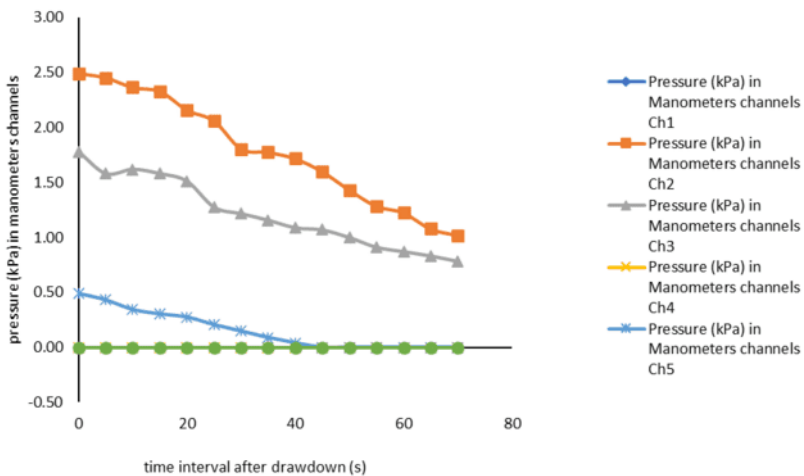


**Figure 15: Pore Water Pressure distribution of model bank in 15.00% moisture content at drawdown ratio 80% H**

*Exploring the impact of water level variations on model river banks composed of different soil types: A flume-based investigation*

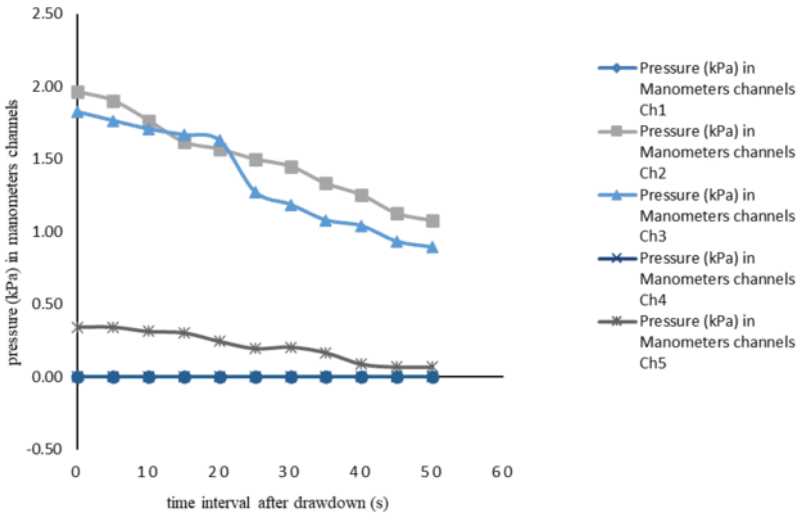


**Figure 16: Pore Water Pressure distribution of model bank in 15.00% moisture content at drawdown ratio 50% H**

Significantly high pore pressure was observed in Channels Ch2 and Ch3, with pressure readings of 2.78 and 2.84 kPa, respectively, for model banks containing 10% moisture content under both drawdown conditions (80%H and 50%H) (Figs. 17 and 18). In contrast, Channels Ch1, Ch4, Ch5, and Ch6 displayed lower pressures of 1.96, 0.54, 0.98, and 0.10 kPa, respectively. However, even after 50 seconds from the drawdown, only a portion of the pressure, ranging from 30% to 40%, dissipated. These results indicate that a moisture content of 10% retains more pore water pressure compared to a moisture content of 15%. Additionally, the dissipation of pressure was slow for both moisture contents. These findings suggest that the river bank, composed of silty clay, exhibited less failure compared to the sandy soil model bank. This can be attributed to the cohesive nature of the silty clay, which plays a crucial role in impeding failure.

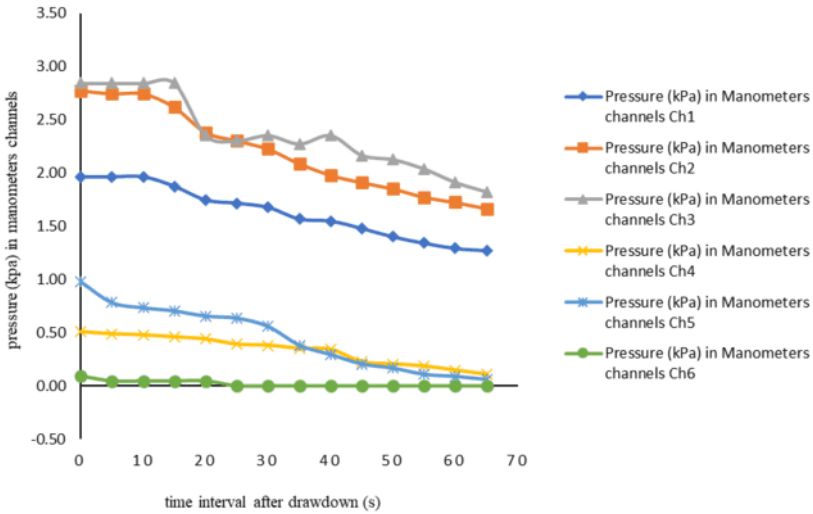


**Figure 17: Pore Water Pressure distribution of model bank in 10.00% moisture content at drawdown ratio 80%H**

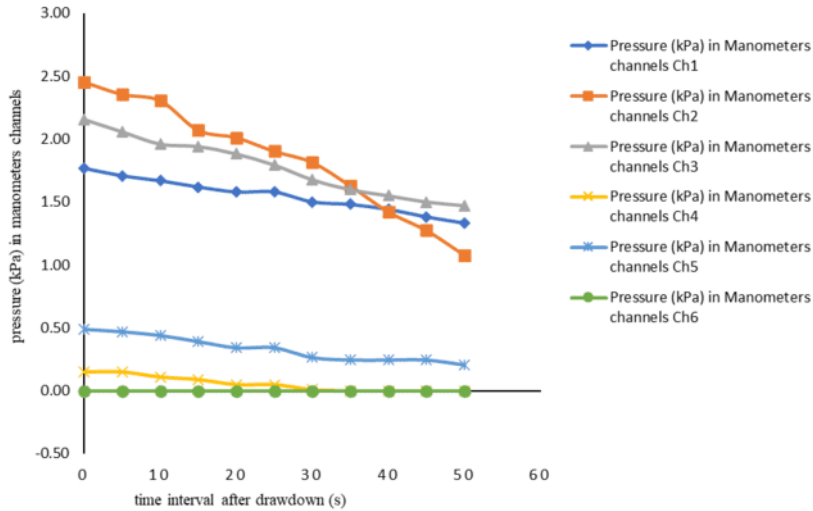


**Figure 18: Pore Water Pressure distribution of model bank in 10.00% moisture content at drawdown ratio 50%H**

The hydrostatic pressure acting on the inclined surface modifies as the simulated river embankment experiences rapid drawdown, leading to a shift in the overall stress distribution within the embankment. As a result, there is a corresponding fluctuation in the pore water pressure attributed to this alteration in stress levels. The pore water pressure's direction and magnitude are contingent upon the flow direction and mechanical

response of the soil matrix. In the current experiment, the bank material of the cohesionless sand model river bank exhibits a relatively high permeability, resulting in a high dissipation rate of pore water pressure. Additionally, the cohesionless soil possesses a minimal particle to particle attractive force, which leads to the dislodgement of soil particles under the pressure of force exerted by pore pressure after the drawdown, causing mass failure of the slope surface. This condition is indicative of a state in which the bank has lost its fluid content. As a result, the behavior of the bank when subjected to drawdown conditions relies on a joint assessment of the drawdown velocity and the bank material's permeability. Additionally, it has been noted that the highest pore pressure in silty clay soil surpasses that in sandy soil. In cohesionless soil, there exists a greater number of inherent seepage pathways, leading to an increased dissipation rate of pore pressure. Conversely, the permeability of silty clay soil is insufficient, causing a diminished dissipation rate of pore pressure.

## **CONCLUSION**

The primary conclusion of this study is presented below.

- 1) Moisture content has exerted a considerable influence on the magnitude of failures. In this investigation, the maximum failure for cohesionless soil was observed under 6% moisture content with an 80%H drawdown. Conversely, the model bank composed of silty clay soil did not exhibit significant failure.
- 2) For both soil types, a 0.5-height drawdown showed no discernible effects on the model bank.
- 3) The results showed a clear pattern in which the failure did not coincide exactly with the decline phase. As an alternative, failures appeared at different times after drawdown began, a process linked to pore water escaping the embankment.
- 4) The findings show that the sand-built model bank has some problems that are comparable to those that are seen in the field.
- 5) The distribution of pore pressure after drawdown at various positions along the bank demonstrates that the highest pressure is maintained within the central channel, as opposed to channels closer to the slope and countryside.
- 6) The results of pore pressure distribution in sandy and silty-clay banks clearly indicate the reasons for the absence of failure or minimal erosion in silty clay banks due cohesive properties of the silty clay bank.
- 7) For sandy banks, maximum failure tends to occur near the channel where the rate of pore pressure depletion is higher post-drawdown.
- 8) Therefore, this investigation demonstrates the feasibility of conducting a physical model analysis prior to the implementation of a bank safeguarding initiative. Within the realm of geo-fluvial simulation, it was observed that the bank constructed using cohesionless soil exhibited a breakdown pattern that closely mirrored real-world scenarios compared to a bank made of cohesive soil across various environmental settings.

### **Declaration of competing interest**

The authors declare that they have no known competing financial interests or personal relationships that could have appeared to influence the work reported in this paper.

### **REFERENCES**

- ACHOUR B., MEHTA D., AZAMATHULLA H. (2024). A New Trapezoidal Flume for Open Channel Flow Measurement Design, Theory, and Experiment, *Larhyss Journal*, No 59, pp. 157-179.
- BERREZEL Y.A. ABDELBAKI C., ROUISSAT B., BOUMAAZA T., KHALDOON A.M. (2023). Decision support system for the management of water distribution networks a case study of Tourville, Algeria, *Larhyss Journal*, No 54, pp. 7-24.
- BOUGAMOUSA A., REMINI B., SAKHRAOUI F. (2020). Analytical study of sediment evolution in the lake of the Fom El Gherza dam (Biskra, Algeria), *Larhyss Journal*, No 43, pp. 169-179.
- CAMAJ A., HAZIRI A., NURO A., IBRAHIMI A.C. (2024). Levels of BTEX and Chlorobenzenes in water samples of White Drin River, Kosovo, *Advanced Engineering Science*, Vol. 4, pp. 45–53.
- CHADEE A., RAMSUBHAG C., MOHAMMED A. (2024). Implications of Bid Rigging Practices in Small Island Developing States: A Case Study, *Asian American Research Letters Journal*, Vol. 1, Issue 4, pp. 1-28.
- CHABOKPOUR J., AZAMATHULLA H.M.D. (2025). Multi-scale CFD analysis of erosion dynamics in heterogeneous rockfill structures implications for sustainable hydraulic engineering design, *Larhyss Journal*, No 61, pp. 217-239.
- CHEN X., HUANG J. (2011). Stability analysis of bank slope under conditions of reservoir impounding and rapid drawdown. *Journal of Rock Mechanics and Geotechnical Engineering*, Vol. 3, pp. 429-437.
- DAS T.K., HALDER H.K., GUPTA I.D. (2017). Impact of riverbank erosion: A case study, *Australasian Journal of Disaster and Trauma Studies*, Vol. 21, Issue 2.
- DUONG THI T., DO MINH D. (2019). Riverbank stability assessment under river water level changes and hydraulic erosion, *Water*, Vol. 11, Issue 12, 2598.
- ERTUĞRUL ÖZGÜR L., İNAL F. (2022). Assessment of the artificial fiber contribution on the shear strength parameters of soils, *Advanced Engineering Science*, Vol. 2, pp. 93–100.
- GASPAROTTO A., DARBY S.E., LEYLAND J., CARLING P.A. (2022). Water level fluctuations drive bank instability in a hypertidal estuary, *Earth Surface Dynamics Discussions*, pp. 1-28.

- GASSI K.A.A., SAOUDI H. (2023). The effect of the physical parameterization schemes in WRF-ARW on the quality of the prediction of heavy rains that cause flooding application on eastern Algeria, *Larhyss Journal*, No 56, pp. 123-137.
- GHOSH D. (2022). Effect of river bank failure on vital social institution ‘marriage’: a case study at Jangipur sub-division of Murshidabad district, West Bengal, India, *Spatial Information Research*, Vol. 30, Issue 5, pp. 647-654.
- ISLAM A., GUCHHAIT S.K. (2021). Social engineering as shock absorbing mechanism against bank erosion: A study along Bhagirathi River, West Bengal, India, *International Journal of River Basin Management*, Vol. 19, Issue 3, pp. 379-392.
- ISLAM M.S., MATIN M.A. (2023). Prediction of fluvial erosion rate in Jamuna River, Bangladesh, *International Journal of River Basin Management*, Vol. 2, Issue 4, pp. 625-637.
- KANA COLLINS E. (2017). An appraisal of the Logone bank dynamics between Maga dam and lake Chad, using satellite imagery, *Larhyss Journal*, No 30, pp. 297-315.
- KANTHARIA V., MEHTA D., KUMAR V., SHAIKH M.P., JHA S. (2024). Rainfall–runoff modeling using an Adaptive Neuro-Fuzzy Inference System considering soil moisture for the Damanganga basin, *Journal of Water and Climate Change*, Vol. 15, Issue 5, pp. 2518-2531.
- KARACA E.O., TANYILDIZI M., BOZKURT N., (2022). Investigation of seismic base isolation systems and their properties, *Engineering Applications*, Vol. 1, Issue 1, pp. 63–71.
- KARAKURT A.B., ERTUĞRUL, ÖZGÜR L. (2023). A laboratory study on the liquid limits of cohesive soils improved with rice hush ash, *Advanced Engineering Science*, Vol. 3, pp. 8–14.
- KARASU V., YALÇIN C., URAS Y. (2023). Geology, geochemistry and isotope compositions of carbonate-hosted barite deposit in Koçaşlı (Gülner-Mersin, Türkiye), *Engineering Applications*, Vol. 2, Issue 1, pp. 75–83.
- KHATUN S., GHOSH A., SEN D. (2019). An experimental investigation on effect of draw-down rate and drawdown ratios on stability of cohesion-less river bank and evaluation of factor of safety by total strength reduction method, *International Journal of River Basin Management*, Vol. 17, Issue 3, pp. 289–299.
- KOUADIO Z.A., SORO G.E., KOUAKOU K.E., GOULA BI T.A., SAVANE I. (2018). Frequent flooding in Agboville (Côte d'Ivoire): what origins? *Larhyss Journal*, No 33, pp. 189-207. (In French)
- KRZEMINSKA D., KERKHOF T., SKAALSVEEN K., STOLTE J. (2019). Effect of riparian vegetation on stream bank stability in small agricultural catchments, *Catena*, Vol. 172, pp. 87-96.
- LI C., YANG Z., SHEN H.T., MOU X. (2022). Freeze-Thaw Effect on Riverbank Stability, *Water*, Vol. 14, Issue 16, pp. 2479.

- MEHDI R., GÜNAL A.Y. (2023). The impact of land use and slope change in flow coefficient estimation, *Engineering Applications*, Vol. 2, Issue 3, pp. 254–264.
- MEHTA D., HADVANI J., KANTHARIYA D., SONAWALA P. (2023). Effect of land use land cover change on runoff characteristics using curve number: A GIS and remote sensing approach, *International Journal of Hydrology Science and Technology*, Vol. 16, Issue 1, pp. 1-16.
- MEHTA D., PRAJAPATI K., ISLAM M.N. (2022). Watershed delineation and land use land cover (LULC) study of Purna River in India, In *India II: Climate Change Impacts, Mitigation and Adaptation in Developing Countries*, Springer International Publishing, pp. 169-181.
- MFOUTOU W., DIABANGOUAYA D.B. (2019). Bank erosion on the Mfilou river on Brazzaville, *Larhyss Journal*, No 39, pp. 299-311. (In French)
- MONDAL S., PATEL P.P. (2020). Implementing Vetiver grass-based riverbank protection programmes in rural West Bengal, India, *Natural Hazards*, Vol. 103, Issue 1, pp. 1051-1076.
- NARDI L., RINALDI M., SOLARI L. (2012). An experimental investigation on mass failure occurring in a river bank composed of sandy gravel, *Geomorphology*, Vol. 163, pp. 56-69.
- NEZZAL F., BELKEBIR R., BENHAIDA A (2015). Risk of flooding in the watershed of the Oued Hamiz (Bay of Algiers), *Larhyss Journal*, No 22, pp. 81-89. (In French)
- OSMAN M.A., THORNE C.R. (1988). Riverbank stability analysis I Theory, *Journal of Hydraulic engineering*, American Society of Civil Engineers, ASCE, Vol. 114, pp. 134–150.
- PANDEY B.R., KNOBLAUCH H., ZENZ G. (2023). Slope Stability Evaluation Due to Reservoir Draw-Down Using LEM and Stress-Based FEM along with Mohr–Coulomb Criteria, *Water*, Vol. 15, Issue 22, Paper ID 4022.
- PAREZ S., KOZAKOVIC M., HAVLICA J. (2023). Pore pressure drop during dynamic rupture and conditions for dilatancy hardening, *Journal of Geophysical Research: Solid Earth*, Vol. 128, Issue 7. <https://doi.org/10.1029/2023JB026396>.
- PARKER C., SIMON A., THORNE C.R. (2008). The effects of variability in bank material properties on riverbank stability: Goodwin Creek, Mississippi, *Geomorphology*, Vol. 101, Issue 4, pp. 533-543.
- REMINI W., REMINI B. (2003). Sedimentation in north African dams, *Larhyss Journal*, No 2, pp. 45-54. (In French)
- REMINI B. (2010). A new approach to fight against dams' siltation: the emerged obstacle technique, *Larhyss Journal*, No 9, pp. 43-53. (In French)
- REMINI B. (2017). A new management approach of dams' siltation, *Larhyss Journal*, No 31, pp. 51-81. (In French)

- REMINE B. (2017). When two opposing ecosystem wet and dry bind by erosion phenomenon? case of the Sahara desert and the amazon forest, Larhyss Journal, No 31, pp. 249-285. (In French)
- REMINE B., TOUMI A. (2017). The Beni Haroun reservoir (Algeria) is it threatened by siltation? Larhyss Journal, No 29, pp. 249-263.
- REMINE B. (2023). Flash floods in Algeria, Larhyss Journal, No 56, pp. 267-307.
- RIABI R., BELAID H., HATIRA A., BACCOUCHE S. (2020). Contribution to the study of runoff and erosion of low slope homogeneous hydrological units of a watershed of the middle valley of Medjerda (Tunisia), Larhyss Journal, No 43, pp. 119-137.
- RINALDI M., CASAGLI N. (1999). Stability of stream banks formed in partially saturated soils and effects of negative pore water pressures: the Sieve River (Italy), *Geomorphology*, Vol. 26, pp. 253-277.
- SAHU R.T., MEHTA D.J. (2024). Impact of coastal inundation due to rise in sea level: A case study of Surat City, India, *Water Practice & Technology*, Vol. 19, Issue 5, pp. 1753-1768.
- SARIF M.N., SIDDIQUI L., ISLAM M.S., PARVEEN N., SAHA M. (2021). Evolution of river course and morphometric features of the River Ganga: A case study of up and down-stream of Farakka Barrage, *International Soil and Water Conservation Research*, Vol. 9, Issue 4, pp. 578-590.
- SEN P. (2008). River bank erosion and protection in Gangetic delta. *River Bank Erosion and Land Loss*, a book published by Visva Bharati Publishing Department, Kolkata.
- SHARMA K.V., KUMAR V., SINGH K., MEHTA D.J. (2023). LANDSAT 8 LST Pan sharpening using novel principal component based downscaling model. *Remote Sensing Applications: Society and Environment*, Vol. 30, pp. 1-15.
- TIWARI B., AJMERA B. (2023). Advancements in Shear Strength Interpretation, Testing, and Use for Landslide Analysis, *In Progress in Landslide Research and Technology*, Vol. 2, Issue 2, pp. 3-54.
- VERMA S., VERMA M.K., PRASAD A.D., MEHTA D.J., ISLAM M.N. (2024). Modeling of uncertainty in the estimation of hydrograph components in conjunction with the SUFI-2 optimization algorithm by using multiple objective functions, *Modeling Earth Systems and Environment*, Vol. 10, Issue 1, pp. 61-79.
- WAIKHOM S.I., YADAV V.K., CHADEE A.A., VARMA V. (2023). Variability in trends of streamflow and precipitation in the Narmada River Basin over the past four decades, *Water Supply*, Vol. 23, Issue 3, pp. 1495-1518.
- ZHOU Y., QU Z., ZHANG W., WANG Z. (2019). SPH simulation on the coupled failure of slope-building adjacent to water triggered by the rapid drawdown of water level, *Mathematical Problems in Engineering*, Vol. 2019, pp. 1-12.  
<https://doi.org/10.1155/2019/8956198>.